ELSEVIER

Atmospheric Research 47–48 (1998) 505–528

ATMOSPHERIC RESEARCH

Simulations of marine stratocumulus using a new microphysical parameterization scheme

Graham Feingold [a,*], R.L. Walko [b], Bjorn Stevens [c], W.R. Cotton [b]

[a] *Cooperative Institute for Research in the Atmosphere / NOAA Environmental Technology Laboratory, 325 Broadway, Boulder, CO 80303, USA*

[b] *Colorado State University, Department of Atmospheric Science, Fort Collins, CO 80523, USA*

[c] *National Center for Atmospheric Research, Boulder, CO 80307, USA*

Abstract

A new microphysical scheme that uses lognormal basis functions to represent cloud and drizzle drop spectra is presented. The scheme is incorporated in a two-dimensional (2-D) eddy-resolving model and applied to the simulation of a stratocumulus cloud deck based on a sounding from the Atlantic Stratocumulus Transition Experiment. Firstly, the philosophy behind the design of the scheme is discussed with emphasis on special problems that arise when simulating stratocumulus clouds. These include (but are not limited to) simulation of collection at low liquid water contents (a few tenths of g m^{-3}), and the importance of correctly simulating drop sedimentation in weakly convective clouds. The scheme is then applied to two cases; one exhibiting weak precipitation (< 1 mm d^{-1} at the surface) and the other, a more strongly precipitating case (1–3 mm d^{-1} at the surface). Results show that the scheme captures the main features of a precipitating stratocumulus system when compared with the same model using a detailed bin microphysical scheme. The new scheme uses less than a fourth of the time required by the bin microphysical model and thus enables one to perform 2-D and 3-D simulations of the cloudy boundary layer over much larger domains, or much longer timescales than was previously possible.

Keywords: Marine stratocumulus; Microphysical scheme; Simulation

1. Introduction

The stratocumulus-capped marine boundary layer has come under increased scrutiny over the past decade through the implementation of three major field

* Corresponding author. Tel.: +1-303-497-3098; e-mail: gfeingold@etl.noaa.gov

0169-8095/98/$19.00
PII S0169-8095(98)00058-1

programs [First ISCCP (International Satellite Cloud Climatology Project) Regional Experiment—FIRE I, Atlantic Stratocumulus Transition Experiment; ASTEX (Albrecht et al., 1995), Southern Ocean Cumulus Experiment; SOCEX (Boers et al., 1996)] as well as a series of modeling workshops that have been aimed at intercomparisons of a host of model results (e.g., Moeng et al., 1996). The models have ranged from one-dimensional (1-D) closure models with simple microphysical schemes (Bechtold et al., 1996) to large eddy simulations (LES) coupled to drop-size resolving microphysical schemes (Stevens et al., 1996a; Kogan et al., 1994, 1995). Each of the models has proven useful in improving our understanding of boundary layer (BL) processes.

The Cloud Physics group at Colorado State University has over the past few years actively pursued use of the LES technique coupled with drop-size-resolving microphysics with the underlying philosophy that it is important to provide a balance between the detail in representation of the BL dynamics and the representation of cloud microphysics (Cotton et al., 1995). In fact, one can broaden this perspective and emphasise the subtle balance between dynamics, microphysics, radiation and even chemistry. These four central components are closely intertwined in myriad ways. A few examples are as follows: BL dynamics drive cloud microphysics by determining the magnitude of the supersaturation field and activation of cloud condensation nuclei (CCN) to droplets (e.g., Twomey, 1959); longwave radiative cooling is a primary driving force of the eddies; drop number concentrations determine droplet size and shortwave radiational heating at cloud top, which in turn affects cloud top cooling and thus the strength of the eddies; CCN particle concentrations determine the colloidal stability of a cloud and the possibility of drizzle formation; drizzling clouds tend to stabilize the BL through evaporative cooling near the surface (Feingold et al., 1996a; Stevens, 1996); aqueous chemistry converts SO_2 to sulfate and generates larger, more easily activated CCN; drop collection reduces the number of CCN and also creates larger particles (Feingold et al., 1996b).

Neglecting one or more of these components (i.e., dynamics, microphysics, radiation and chemistry) necessarily means compromising the results in some way or another and it is therefore incumbent upon the researcher to apply a model that is adequate for studying the problem at hand. Current three-dimensional (3-D) LES models (Stevens et al., 1996a; Kogan et al., 1995) are unable to include all of the abovementioned processes over domain sizes larger than a few kilometres (about 50^3 grid points) and for integration times longer than 3 or 4 h. The enormous computational expense of these models is due to the size resolving microphysics (termed bin-microphysics in this work). There are two sources: the first is simply due to the additional 50 or so predictive equations that are needed to represent the drop size distribution; the second is due to the expense of the microphysical calculations themselves. When faced with these restrictions, many have opted for simple microphysical parameterizations (e.g., Kessler, 1969; Berry, 1967; Berry and Reinhardt, 1974, etc.) comprising a few simple algebraic equations to represent droplet growth through the autoconversion process, and raindrop growth through the accretion process. Drop sedimentation is also parameterized in a simple fashion. In the case of LES of stratocumulus, the trend has been to ignore microphysics altogether and just use saturation adjustment diagnoses of cloud water, or more recently, application of a modified Kessler scheme (Wyant et al., 1997). It is not

the intent of this paper to fault research emanating from models that use such simple schemes since in many cases, the focus of those works has been on BL processes that were not affected by cloud microphysics. A case in point is the nocturnal, non-drizzling boundary layer (e.g., Moeng, 1986). However, when one is concerned with drizzling boundary layers, the onus placed on microphysics is great and simple schemes are not able to capture cloud and BL evolution adequately (e.g., Feingold et al., 1996a; Stevens, 1996). Two examples are recapitulated here to illustrate the point.

(i) In stratocumulus clouds, the importance of autoconversion relative to accretion is greater than it is for deep convective clouds (Cotton and Anthes, 1989). Because in-cloud up/downdraughts in stratocumulus are only on the order of 10 s of cm s^{-1} to 1 or 2 m s^{-1}, larger, precipitation sized drops tend to fall out of the cloud rapidly. [1] This then reduces the relative importance of the accretion process (drizzle drops collecting cloud drops).

(ii) As pointed out by Feingold et al. (1996a), the sedimentation process is also important if one is to represent drizzling boundary layers with integrity. Typically, bulk microphysical schemes predict on water mass, and, occasionally also on drop number concentration. These schemes typically assign one mean fall velocity to all precipitation, with a value determined either arbitrarily (if no size information is available), or based on the mass-mean diameter. In reality, each drop falls at its own terminal velocity and the vertical distribution of water is different from that obtained using such a bulk method. The sensitivity of sedimentation to this assumption will be investigated in this work.

The goals of this work are three-fold: Firstly, we consider extant microphysical parameterizations and discuss their shortcomings for stratocumulus studies. Secondly, we present a new microphysical parameterization scheme that attempts to capture the essence of the detailed bin microphysics, but with much smaller computational expense. Preliminary results (Olsson et al., 1996) were sufficiently promising so as to encourage further development of this approach. Thirdly, this scheme is applied in a simulation of a drizzling stratocumulus cloud deck based on a recent GEWEX Cloud System Studies (GCSS) workshop case study from the ASTEX experiment (Duynkerke et al., 1995) and comparisons are made with a full bin microphysical model.

2. The dynamical model

The dynamical model used in this study is the LES version of the Regional Atmospheric Modeling System (RAMS) model developed at Colorado State University (Pielke et al., 1992). In this study it is used in its two-dimensional (2-D) form, and is therefore more appropriately termed an eddy resolving model (ERM), rather than an LES model. It has been applied to stratocumulus studies in both LES and ERM form in a number of works (Feingold et al., 1994, 1996a,b; Stevens et al., 1996a; Stevens, 1996) that have investigated various aspects of CCN–cloud interactions and drizzle formation. A critical analysis of the model and the LES technique can be found in the work of

[1] e.g., a 50-μm radius drop has a fall velocity of about 27 cm s^{-1}.

Stevens et al. (1996a). The model is nonhydrostatic and compressible. Predictive equations are solved for two velocity components (u,w), liquid–water potential temperature, θ_l, perturbation Exner function π, and total water-mixing ratio r_t. The model includes sophisticated short and longwave radiation schemes that are fully coupled with the rest of the model. In the current study, however, only a simple longwave radiation scheme dependent on cloud liquid water content is used, and no shortwave is simulated. This is in accordance with the GCSS case study prescribed for a recent workshop as described later in the text.

In prior studies, the RAMS model has been coupled with a variety of microphysical models exhibiting varying degrees of complexity. These range from simple saturation adjustment schemes where all excess vapor above saturation is condensed, through the use of simple representations of microphysics (both water and ice), and, to the more sophisticated bin microphysics (Feingold et al., 1994). In this paper we describe a new scheme that is aimed at bridging the gap between the simple schemes and the accurate, but expensive, bin microphysics.

3. Description of extant microphysical schemes

3.1. Autoconversion and accretion

Many warm cloud models use simple autoconversion and accretion schemes based on the works of Berry (1967), Kessler (1969), and Berry and Reinhardt (1974); Berry and coworkers formulated their parameterizations in terms of cloud drop mass, number and spectral breadth while the Kessler parameterization is based on water mass only. More recently Beheng (1994) has also proposed a scheme based on mass, number and spectral breadth. A comparison of these schemes with a detailed bin model (Tzivion et al., 1987) shows great disparity in autoconversion rates between the abovementioned schemes, and none perform well (compared with the bin model) for the low liquid water content (< 1 g m^{-3}, and frequently < 0.5 g m^{-3}) regime associated with stratus clouds. Indeed this comes as no surprise since these schemes were never designed with stratiform clouds in mind in the first place. For example, the lower cutoff liquid water content for both Kessler (1969) and the schemes of Beheng (1994) is 0.5 g m^{-3}, and many stratocumulus and stratus have liquid water contents of only a couple of tenths of g m^{-3}. There are also some indications that autoconversion schemes perform poorly at high LWCs (> 3 g m^{-3}). The current study is not directly concerned with these cases but the proposed technique is generally applicable to all LWC situations.

The abovementioned schemes (excluding the work of Kessler, 1969) have in common the fact that simple functions have been fit to data based on bin model calculations of collection in a closed box. This approach suffers from the problem that the fit is by necessity a compromise and the simple equation is not able to adequately represent all possible realisations.

It is thus clear that a parameterization scheme that bridges the gap between simple autoconversion/accretion schemes and bin microphysical models is required, and moreover, that it be designed for the range of possible scenarios encountered in clouds —including stratiform clouds. The direction of research explored in this work is based

on the work by Clark (1976) who used basis functions (lognormal or gamma) to describe the cloud and raindrop spectra. In that work, the techniques were applied in box-models so that dynamical processes were not represented. Nevertheless, the first steps of the current research can be found therein.

The main concept behind this approach is that the cloud and rain (or drizzle) spectra are each represented by a basis function such as the lognormal or gamma function. In a dynamical model, this requires a total of four to six prognostic variables to describe the two basis functions (four if the breadth parameter is fixed and, six if the breadth is allowed to vary). Typically this means predicting on either 2 or 3 moments of each of the size spectra; mass and number are the prime candidates and, if spectral breadth is required, surface area, or radar reflectivity (the 6th moment with respect to diameter) can be solved for. Feingold et al. (1994) applied this technique to representation of the CCN spectrum and the reader is referred to the Appendix of that work for details. An important point raised in that work was that a monotonic advection scheme is a prerequisite with this type of microphysical representation; if not, the mean drop-mass calculated from the ratio of mass to number may lie beyond the reasonable range and, retrieval of the breadth parameter, which is based on a ratio of the three predicted moments, can in some instances (e.g., at sharp gradients) be non-physical.

Clark (1976) described the cloud and rain spectra by lognormal functions. In calculating the tendencies on the moments of these functions, look-up tables were built for truncated lognormal spectra convolved with the kernel function for cloud–cloud or rain–rain interactions. Solution proved cumbersome, but nevertheless tractable for cloud–rain interactions where the integrand had to be approximated by a high-order polynomial. In this work we use a different approach which emphasises the importance of including detailed information on drop–drop interactions over discrete bins.

The general moment equation for a drop spectrum $n(m)$ is given by

$$\frac{\mathrm{d}M^j}{\mathrm{d}t} = \frac{1}{2}\int_0^\infty (x+m)^j \mathrm{d}x \int_0^\infty n(x)\, n(m)\, K(x,m)\mathrm{d}m - \int_0^\infty m^j n(m)\mathrm{d}m \int_0^\infty n(x)\, K(m,x)\mathrm{d}x, \tag{1}$$

where M^j represents the jth moment of the spectrum, and $K(m,x)$ is the collection kernel for a drop of mass m interacting with one of mass x. For clarity in presenting the following concepts the region of integration has been defined as $(0; \infty)$ and only one size distribution $n(m)$ [or $n(r)$, where r is drop radius], defined over the aforementioned range is used. The concepts are easily mapped to the case of two or more spectra defined in subranges with the addition of some book-keeping of mass and number transfer from one range to the other (i.e., cloud to drizzle). Dividing mass space into bins $(x_k; x_{k+1})$ (e.g., Yair et al., 1994) yields

$$\frac{\mathrm{d}M^j}{\mathrm{d}t} = \frac{1}{2}\sum_{i=1}^{I}\sum_{k=1}^{I}\int_{x_i}^{x_{i+1}} (x+m)^j \mathrm{d}x \int_{x_k}^{x_{k+1}} n_i(x)\, n_k(m)\, K_{i,k}(x,m)\mathrm{d}m - \sum_{i=1}^{I}\sum_{k=1}^{I}\int_{x_k}^{x_{k+1}} m^j n_k(m)\mathrm{d}m \int_{x_i}^{x_{i+1}} n_i(x)\, K_{i,k}(m,x)\mathrm{d}x. \tag{2}$$

For number ($j = 0$), we have

$$\frac{\mathrm{d}N}{\mathrm{d}t} = -\frac{1}{2}\sum_{i=1}^{I}\sum_{k=1}^{I}\int_{x_k}^{x_{k+1}} n_k(m)\,\mathrm{d}m \int_{x_i}^{x_{i+1}} n_i(x)\,K_{i,k}(m,x)\,\mathrm{d}x \tag{3a}$$

and for mass ($j = 1$),

$$\frac{\mathrm{d}M}{\mathrm{d}t} = 0. \tag{3b}$$

We discuss two approaches to solving Eqs. (3a) and (3b); because the infinite spectrum has been divided into bins, both have the advantage that the detailed bin-by-bin transfer rates $K_{i,k}(m,x)$ are used to represent the collection process. This should be contrasted with other schemes that use mean properties of the spectrum (defined over a large size range) to determine mass transfer rates.

3.1.1. Approximate kernel in a bin

Yair et al. (1994) used an approach based on the work of Tzivion et al. (1987) and approximated the kernel function within a bin using a polynomial function. If

$$K_{i,k}(m,x) = \bar{K}_{i,k}(m+x) \tag{4}$$

then

$$\frac{\mathrm{d}N}{\mathrm{d}t} = -\frac{1}{2}\sum_{i=1}^{I}\sum_{k=1}^{I}\bar{K}_{i,k}[M_i N_k + M_k N_i]. \tag{5}$$

This approach greatly simplifies the solution (at least using Eq. (4)) but requires look up tables for M_k; N_k. If truncation tables are not used, calculations become prohibitively slow as incomplete gamma functions or error functions have to be calculated for all bins, at every time step and every grid point. Note that Yair et al. (1994) used a single gamma distribution function to describe $n(m)$ over the range $(0; \infty)$, but solved for three moments of the distribution in order to predict on spectral breadth. The formation of drizzle or rain suggests that use of two basis functions to describe each of the cloud and drizzle spectra is more appropriate than using a single basis function for both.

3.1.2. Direct look-up table for tendencies

This is the approach adopted in this work. In order to obtain the bin-by-bin mass transfer rates, the output from a stochastic collection bin model is used in a form that provides tendencies on cloud mass M_c, cloud number N_c, rain mass M_r and rain number N_r. (Here we refer more specifically to the case of two drop spectra over the size-range). [2] A look-up table of these tendencies is created a priori for a range of feasible physical realisations of the four parameters. The stochastic collection model of Tzivion et al. (1987) is used with a bin resolution based on mass doubling from one bin

[2] In this paper, we will predict on only four parameters and fix the breadth of both the cloud and rain spectra. Also we have opted for the lognormal basis function but believe that the gamma distribution is also a viable candidate.

to the next. Two kernel functions have been used, one based on the work of Long (1974) and the other from Hall (1980); the former will be used throughout. Differences resulting from these two kernels are on the order of 20–30% in precipitation rates (Stevens, 1996).

In principle, any detailed (bin) collection model can be used to generate look-up tables at the required accuracy. Unlike the first approach, approximation to the kernel function is not required. In the case of this work, the stochastic collection model of Tzivion et al. (1987) *does* approximate the kernel in a bin (to facilitate solution of the moment equations), but this is purely incidental. The method is very fast and simple. The look-up table is read in once only; At subsequent time steps, location of table values is derived from a simple algebraic equation, as are the tendencies themselves. A more detailed description of how the look-up tables are built can be found in Appendix A.

This approach is in essence similar to that used by Beheng (1994) and the earlier work of Berry and Reinhardt (1974). It differs only in that no attempt is made here to fit an analytical function to the data set, but instead the complete data set is stored in a table and used on demand.

3.2. Sedimentation

Since both the cloud droplet and raindrop spectra are fully described with the basis function, the sedimentation process consists of dividing the spectrum into individual bins and allowing each bin to fall at the appropriate velocity. The authors have not seen this approach applied elsewhere to sedimentation but it is a logical extension of the concepts outlined for collection. Division of the spectrum into bins requires the calculation of error functions, or incomplete gamma functions, for lognormal and gamma basis functions, respectively. Since these need to be calculated at every grid point and every time step, the process is very expensive. Here, division of the spectrum into bins is done a priori for a range of mean drop sizes (and breadth parameters) and stored in look-up tables. In fact the approach can be extended even further by a priori performing the truncation, sedimentation of each bin according to the terminal velocity of its droplets, and remapping of the mass and number of all bins onto the model grid cells, and then storing this information in look-up tables. For further details see Appendix B.

Drop sedimentation can be calculated using any desired sedimentation (advection) scheme. In this work we have followed our prior work (Feingold et al., 1996a) and used a simple forward scheme that is monotonic and conservative. This was deemed most appropriate since we will be performing comparisons with calculations using the full bin microphysical scheme used in that study. However, it is stressed that other schemes such as the semi-Lagrangian scheme are easily used in conjunction with this approach. Since semi-Lagrangian schemes are desirable for many model scenarios, look-up tables have also been derived for the latter (Appendix B), although they are not used here.

3.3. Condensation / evaporation

Only brief mention is made of this process since it is solved in the same fashion as in the work of Clark (1976). It is noted that this approach is simpler than that adopted for

collection and sedimentation because the spectrum is not sub-divided into bins. The equation for condensation is given by

$$\frac{\partial n(m,t)}{\partial t} = -\frac{\partial}{\partial m}\left[n(m,t)\left(\frac{\mathrm{d}m}{\mathrm{d}t}\right)_{\mathrm{cond/evap.}}\right] \tag{6}$$

where in its simplest form we can write

$$\frac{\mathrm{d}m}{\mathrm{d}t} = \bar{f}(\overline{m})C(P,T)Sm^{1/3}. \tag{7}$$

$C(P,T)$ is a known function of temperature T and pressure P, and S is the supersaturation. Inclusion of gas-kinetic effects does not change the formulation of the equations substantially; see the work of Clark (1976) for details. At this stage, we have not included the gas-kinetic effects. For evaporation, the ventilation coefficient is given by

$$\bar{f} = C_1 + C_2\overline{m}^{1/3}; \quad \overline{m} = \frac{M}{N} \tag{8a}$$

where C_1 and C_2 are constants, while for condensation,

$$\bar{f} = 1. \tag{8b}$$

The moment equations are given by

$$\begin{aligned} &\frac{\mathrm{d}N}{\mathrm{d}t} = 0; \\ &\frac{\mathrm{d}M}{\mathrm{d}t} = \bar{f}C(P,T)S\int_0^\infty m^{1/3}n(m)\mathrm{d}m \end{aligned} \tag{9}$$

Since

$$\int_0^\infty m^{1/3}n(m)\mathrm{d}m \propto \int_0^\infty rn(r)\mathrm{d}r,$$

use of a basis function for $n(r)$ closes the system of equations.

Finally, it is worth mentioning that calculation of the supersaturation field following the semianalytical method of Clark (1973) is easily incorporated into this version of the model since the essential microphysical information (the integral radius) is available, just as it is in the bin-microphysical version.

4. Results

4.1. Model setup

The case study used in this work is based on a boundary layer with drizzling stratocumulus observed during the first Lagrangian experiment in the ASTEX (Albrecht et al., 1995; Bretherton and Pincus, 1995a; Bretherton et al., 1995b). This case was recently modeled by a number of groups during the 3rd GCSS intercomparison

workshop and Fourth International Cloud Modeling Workshop held in Clermont-Ferrand, August 1996. Data were taken from flight A209 (UK Meteorological Research Flight C130) and have been analysed and described in detail in the work of Duynkerke et al. (1995); however due to the idealised form of the initial conditions and forcing, this paper will not address model/data intercomparisons. A 3-h long simulation was proposed, starting at 0400 UTC June 13, 1992 but we extended the simulations to 6 h. To facilitate intercomparison, a number of simplified parameterization schemes were used. The longwave radiative scheme is given by

$$F_L(z) = Ce^{-a\mathrm{LWP}} \tag{10}$$

where $C = 74$ W m^{-2} is the longwave cooling at cloud top, $a = 130$ m^2 kg^{-1} a constant, z_t ($= 1500$ m) the top of the model domain and LWP the liquid water path. The large scale divergence is specified at 5×10^{-6} s^{-1}. Shortwave radiation is not simulated. In addition, geostrophic winds and a surface flux formulation are specified. In the current simulations, however, the surface parameterization based on that of Louis (1979) is used instead of the specified forcing. The grid spacing is 25 m in the vertical and 50 m in the horizontal. The time step is 2 s.

The CCN spectrum is specified as a lognormal function composed of ammonium bisulfite, a total number concentration of 150 cm^{-3}, median radius of 0.1 μm and geometric standard deviation of 1.5. This distribution is assumed to be constant with time. Activation is such that the number of cloud drops cannot exceed the total number of CCN (e.g., Stevens et al., 1996a). No attempt is made here to simulate the depletion in CCN due to collection as was done in the work of Feingold et al. (1996b). The first basis function describing cloud droplets spans the region 1.5 μm; 25 μm (radius); the second function spans the region 25 μm; 500 μm. Each function has a prescribed geometric standard deviation σ_g of 1.2 (equivalent to a relative dispersion of 0.18).

In order to illustrate the application of this microphysical scheme we perform a number of tests and comparisons with the full bin microphysical scheme. This model has been described in detail elsewhere (e.g., Feingold et al., 1994; Stevens et al., 1996a) and will not be belaboured here. Suffice it to say that it is our most accurate representation of cloud microphysical processes based on the moment conserving approach used by Tzivion et al. (1987) and thus represents a modeler's 'ground-truth' for the intercomparison with the new scheme. The runs are first performed using the baseline 150 cm^{-3} CCN particles for both parameterized and bin microphysical schemes. They are then repeated for a CCN concentration of 75 cm^{-3}. For brevity we use the following terminology to differentiate between the schemes: P150 indicates the use of the parameterized microphysics with 150 CCN cm^{-3}; P75 indicates the parameterized microphysics with 75 CCN cm^{-3}. The bin microphysical counterparts are termed B150 and B75, respectively.

4.2. Weak drizzle

Fig. 1 shows a time evolution of domain average fields for the P150 and B150. The fields plotted are (a) liquid water path, LWP [g m^{-2}], (b) root-mean-square vertical velocity, (c) cloud top, z_i, and (d) surface drizzle [mm d^{-1}], with the solid lines

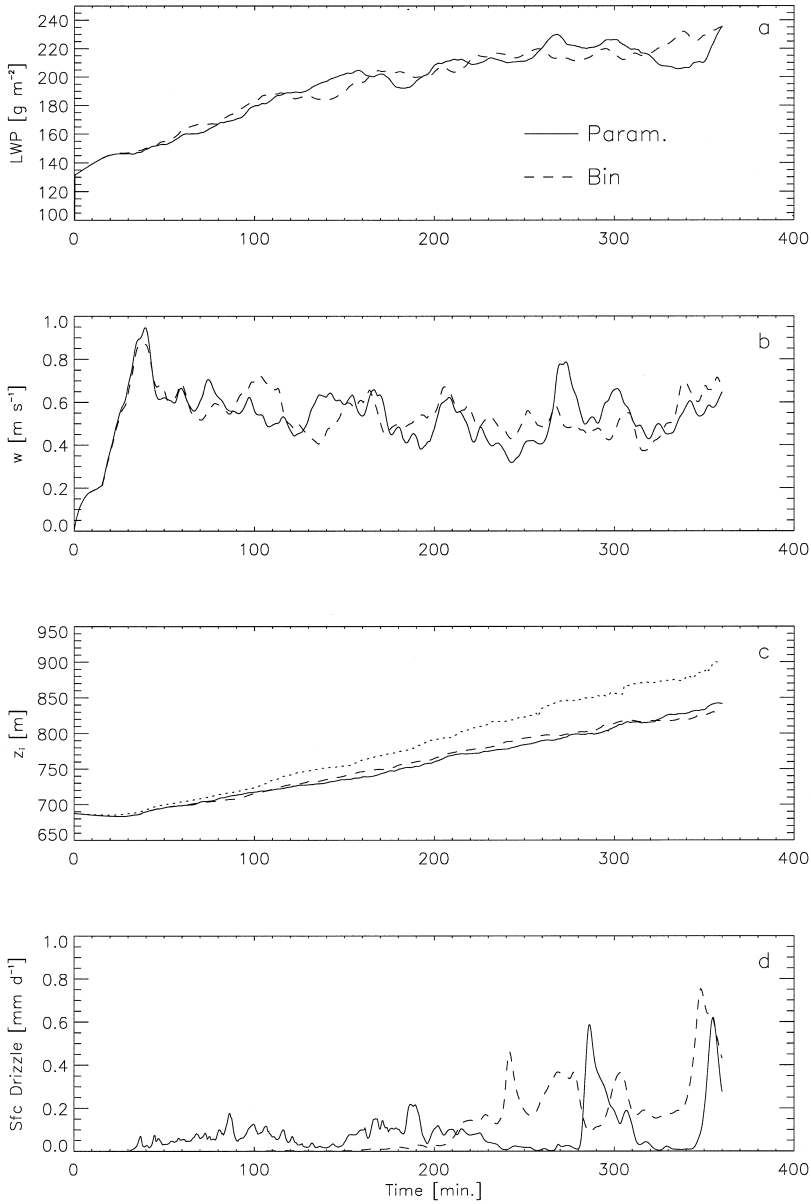

Fig. 1. The temporal evolution of (a) LWP, (b) root-mean-square vertical velocity, (c) cloud top, and (d) surface drizzle for the weak drizzle runs. Solid lines indicate parameterized microphysics and long-dashed lines, bin microphysics. Superimposed on (c) is a short-dashed line indicating the solution for the same run without representation of collection and sedimentation.

indicating the parameterization and dashed lines, the bin model. It is seen that there is generally good agreement between the fields. Most fields exhibit only minor variations from the bin solution, particularly if one looks at the mean values. Also superimposed

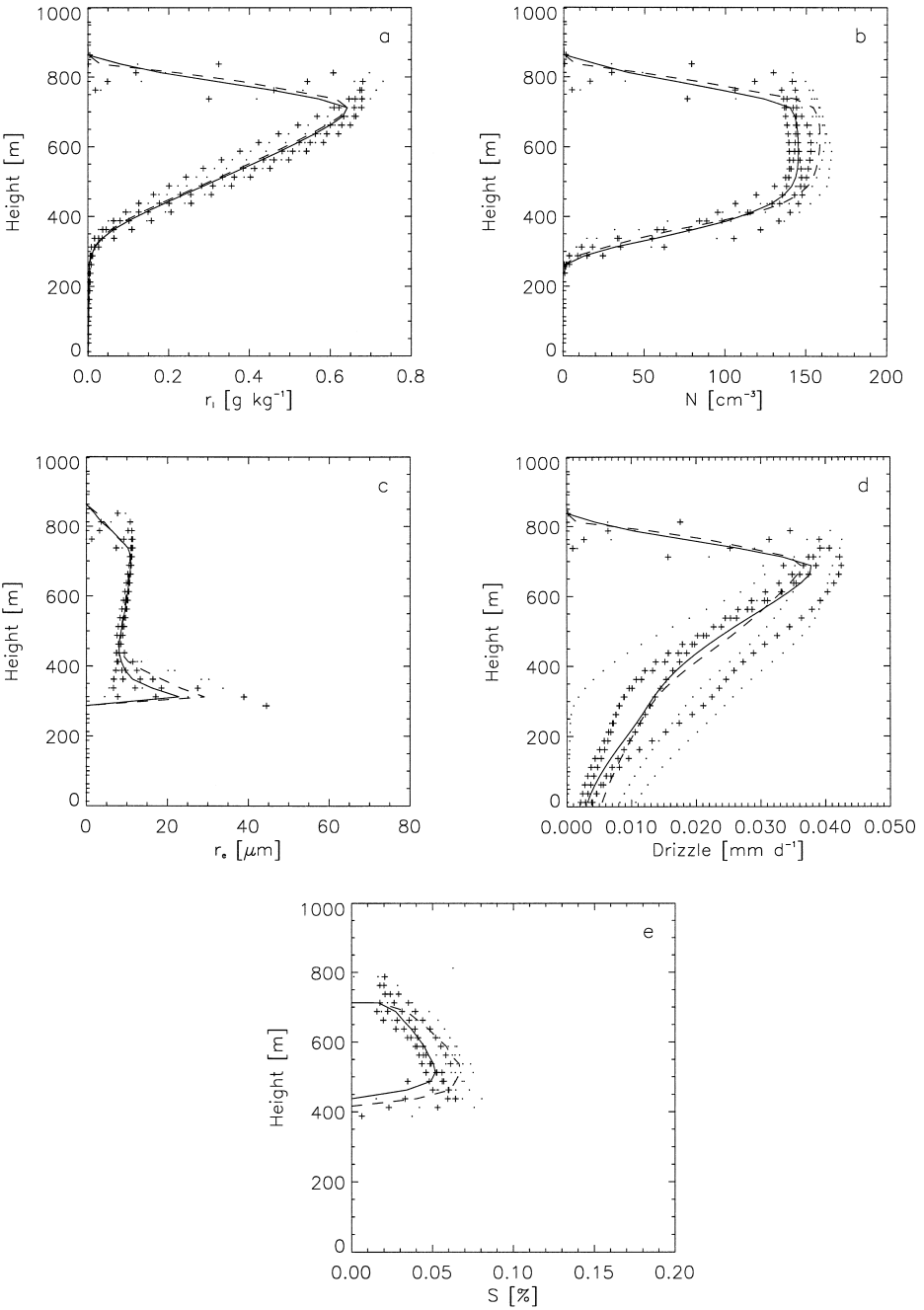

Fig. 2. Temporally and spatially averaged profiles of (a) r_l, (b) N, (c) r_e, (d) drizzle rate, and (e) updraught averaged supersaturation S for the weak drizzle runs in Fig. 1. Symbols indicate individual 1-h averages that go into making the line profiles; '+' indicates the parametrization and '·' the bin microphysics.

on Fig. 1c is the value of z_i from a simple saturation adjustment scheme that does not represent microphysical processes. Clearly the impact of even small amounts of drizzle is not negligible and results in a less rapid increase in z_i. The surface drizzle rate indicates a tendency of the P150 to generate drizzle too early in the simulation, as reflected in a slightly lower LWP during the first two h of the run. The mean surface drizzle rate for P150 is 0.08 mm d^{-1} compared with 0.11 mm d^{-1} for B150.

It is worth bearing in mind that one cannot expect a very good match in values in the temporal sense since small variations in conditions at the beginning of the run can evolve into large differences with time. For this reason, results for layer-averaged mean properties are shown as an average over the last 4 h of the simulation in Fig. 2. To give a sense of the variability in results, individual 1-h averaged profiles are plotted as data points ('+' for P150 and '·' for B150). The 4-h average profiles of (a) cloud water r_l [g kg^{-1}], (b) drop number concentration N [cm^{-3}], (c) drop effective radius r_e [μm], (d) drizzle flux [mm d^{-1}], and (e) updraught-averaged supersaturation S [%] generally show

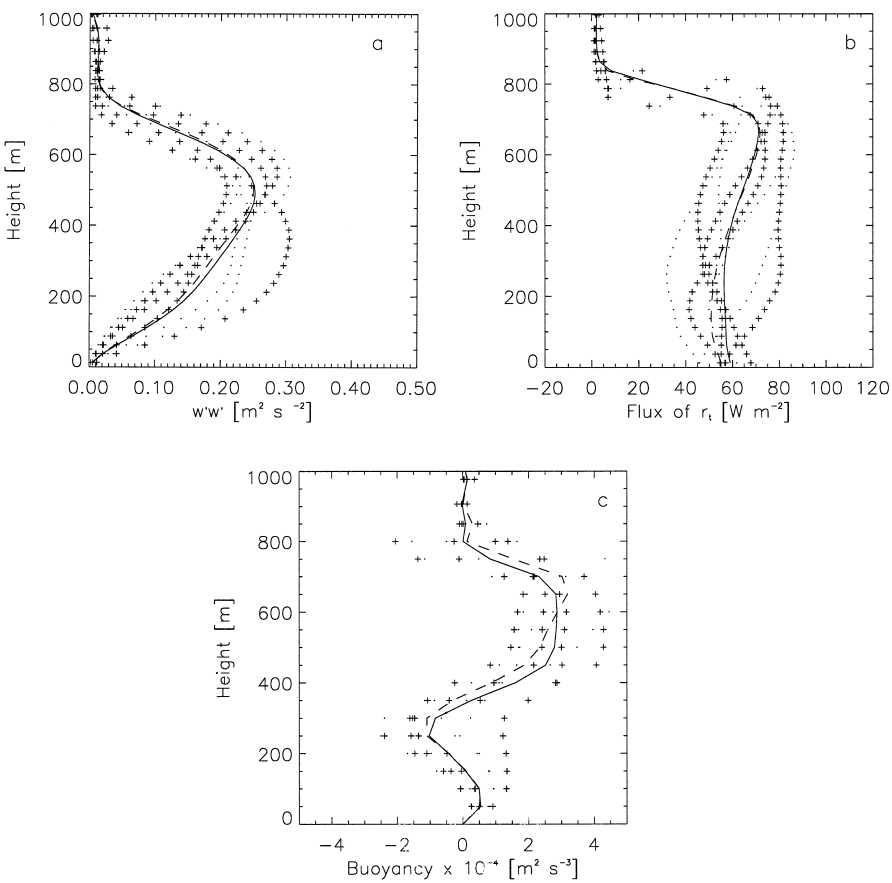

Fig. 3. Temporally and spatially averaged profiles of (a) $w'w'$, (b) flux of total water (vapor + water), and (c) buoyancy contribution to TKE. Line types and symbols are consistent with those in Fig. 2.

excellent agreement with the bin model. There is a tendency for P150 to underpredict drop concentration, and this is consistent with the lower updraught-average supersaturations (Fig. 2e). There is indication that this is at least partially related to the lack of inclusion of gas kinetic effects in P150; these effects retard the growth of the smallest drops, allow supersaturations to build up and result in higher drop concentrations (e.g., Stevens et al., 1996a). The drizzle flux profile (Fig. 2d) is worthy of mention in that it exhibits the same shape as that of the run with bin microphysics.

The r_e profile agrees very well within the main body of the cloud (400–800 m) but B150 shows larger values of r_e at cloud base (300 m). Values of r_e are not plotted for $r_l < 0.01$ g kg^{-1} because at vanishing small amounts of water, the calculation becomes meaningless. Some difference in r_e is to be expected because there are differences in the manner in which r_e is calculated: in the case of the parameterized microphysics, we combine the mass and number from both basis functions into one to calculate r_e, whereas in the bin model the bin information is available to calculate the more correct volume to surface area ratio.

Fig. 3 shows similar layer and time averaged profiles of (a) $w'w'$ (the vertical contribution to turbulence kinetic energy TKE), (b) the flux of total water (liquid plus vapor), and (c) the buoyancy production of TKE. Again, individual 1-h averages are superimposed to indicate the degree of variability. The agreement in both the shape and magnitude of these profiles is excellent, providing further support for the proposed parameterization scheme.

4.3. Stronger drizzle

Similar experiments were repeated with half the CCN concentration (75 cm^{-3}); all other input parameters remained unchanged. These are indicated by P75 and B75 for the parameterization and bin microphysics, respectively. Fig. 4 shows plots of the temporal evolution of various parameters similar to Fig. 1. Here, the LWPs (Fig. 4a) agree to within 4% over the 6 h run (184 g m^{-2} for P75 and 177 g m^{-2} for B75), although P75 loses less water to precipitation than B75 (Fig. 4d) over the last hour. The mean precipitation rates at the surface are 0.54 mm d^{-1} for B75 and 0.32 mm d^{-1} for P75. The timing of the onset of drizzle is reasonable but peak values are somewhat lower for P75. Also, it is noted that whereas in Fig. 1, the drizzle at the surface in P150 preempted that of B150, the reverse is true in this case. Root-mean-square velocities w (Fig. 4b) compare well, as does the cloud top, z_i (Fig. 4c). The strong drizzle events in B75 between 270 and 300 min are correlated with the beginning of a decline in LWP (relative to P75), followed by a decrease in w (relative to P75) as cooling and moistening stabilize the sub-cloud layer (e.g., Stevens, 1996). Profiles of total water flux, $w'w'$ and buoyancy production of TKE bear this out (see Fig. 6).

Profiles of temporally and spatially averaged microphysical fields are shown in Fig. 5 in an analogous manner to Fig. 2. Again, there is generally very good agreement between the parameterization results compared with the bin results, particularly for r_l, N and S fields. Drop effective radii for P75 are excellent in-cloud and show the same qualitative features below the cloud. Although the average drizzle profile for P75 is qualitatively good, it tends to peak lower in the cloud than B75 and have smaller

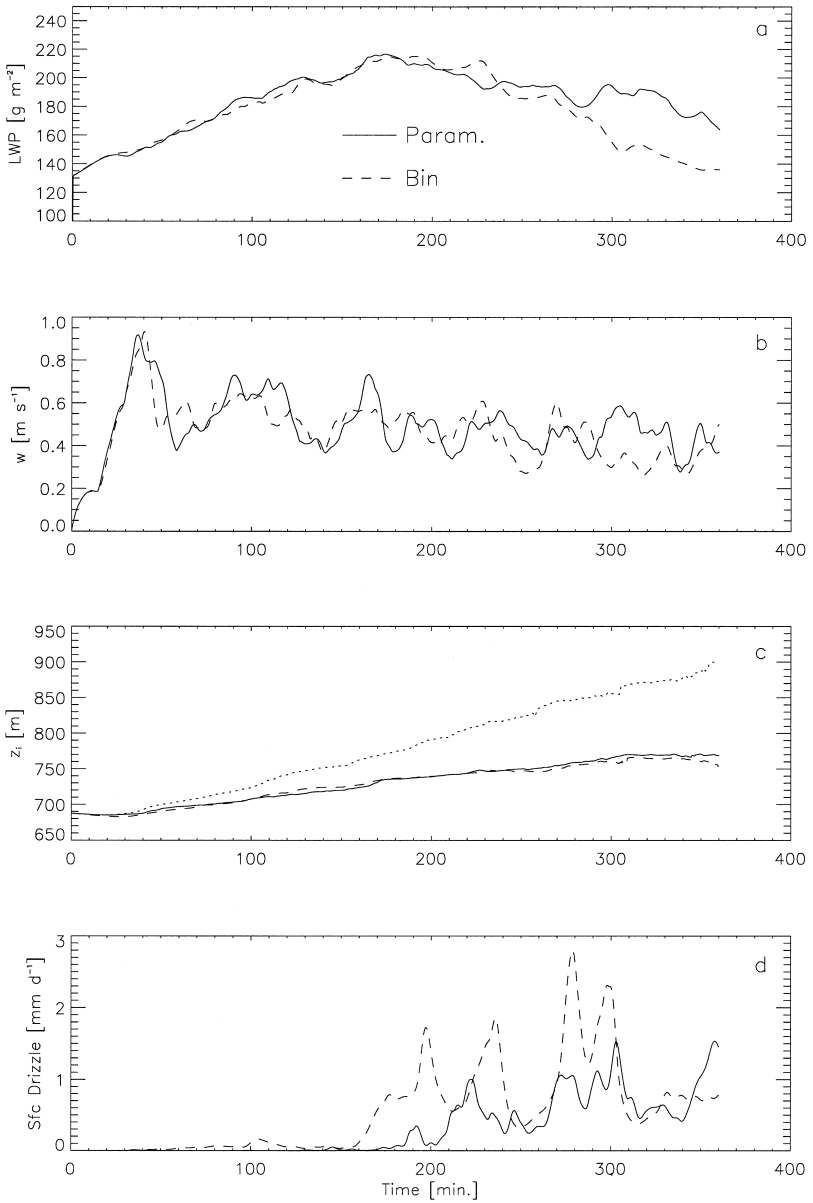

Fig. 4. As in Fig. 1 for the stronger drizzle case.

average surface values (see also Fig. 4d). Supersaturation profiles are similar although peak values are smaller than for B75 and displaced a little lower. P75 also does not have the same degrees of extrema in S evident at cloud base and top in the 1-h data points for B75. Stevens et al. (1996b) have discussed the source of these spurious cloud-top supersaturations.

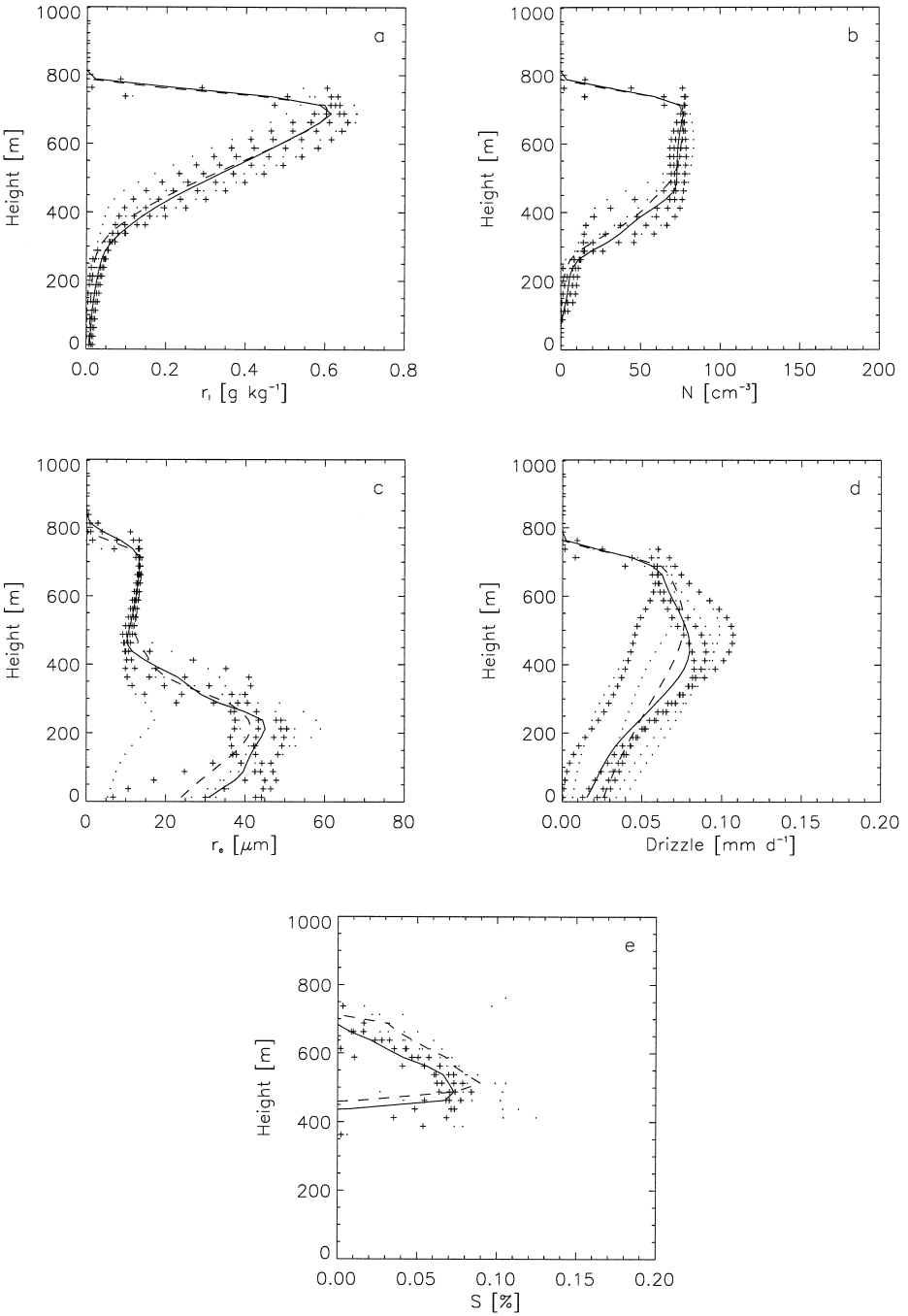

Fig. 5. As in Fig. 2 for the stronger drizzle case.

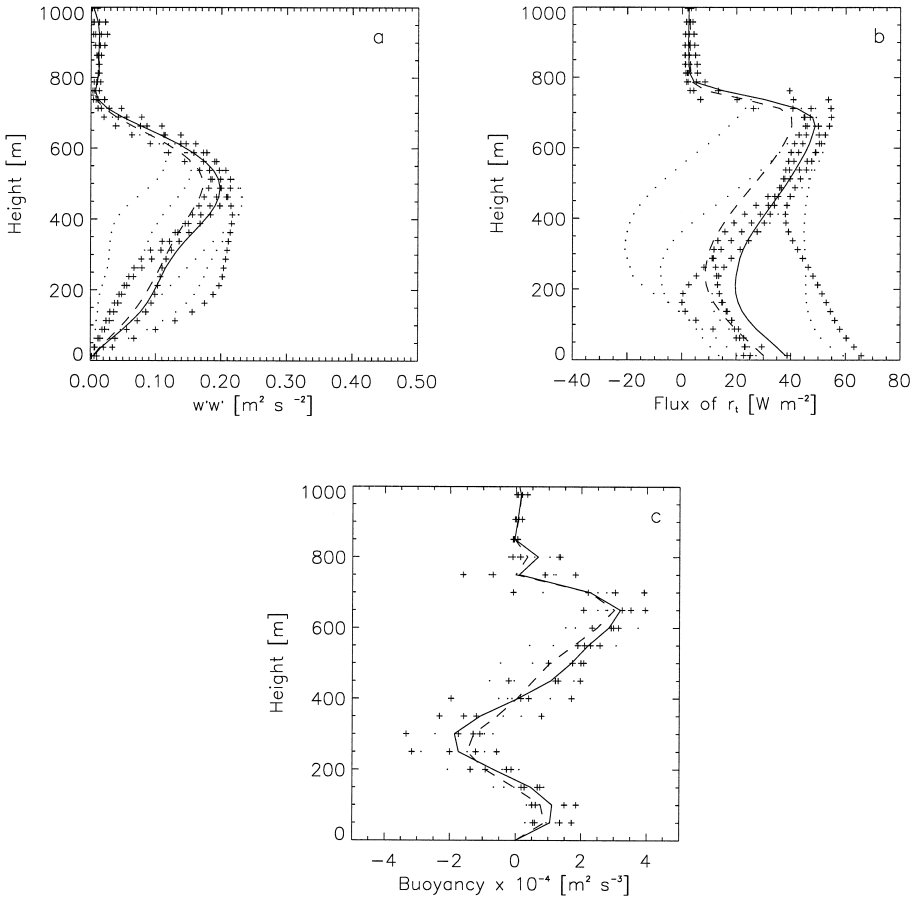

Fig. 6. As in Fig. 3 for the stronger drizzle case.

The mean profiles of $w'w'$ are shown in Fig. 6a. Note that these profiles exhibit weaker turbulence when compared with the weak drizzle case (cf. Fig. 3a). Comparison of parameterized and bin microphysics profiles show good agreement, although values for P75 tend to be larger owing to the weaker drizzle. The general shape of the $w'w'$ profile for P75 does exhibit the correct features—namely depressed values below cloud base where buoyancy production of TKE is negative (Fig. 6c). When comparing this case with the weak drizzle case in Fig. 3 it is clear that buoyancy production of TKE is lower—again a consequence of the stabilizing effect of precipitation. The profiles of buoyancy production of TKE for B75 and P75 show good agreement, with a trend to larger values in the cloud, and smaller values below cloud for P75. Finally Fig. 6b shows that the parameterization successfully captures the qualitative features of the total water flux profile. The B75 run tends to moisten the subcloud layer more than P75, owing to the stronger drizzle, evaporation, and sub-cloud cooling exhibited by B75 in comparison to P75.

5. Discussion

The results presented in Section 4 indicate that the proposed approach to representing microphysical processes in stratocumulus clouds is a viable one. The agreement between model runs using the bin microphysical approach, and with the parameterization is good, with the exception perhaps of the timing and exact magnitude of the drizzle events.

A few words on intercomparison of these runs is in order: Owing to the dynamic nature of the BL system being modeled we cannot expect a good temporal match between bin and parameterized microphysical runs. Slight differences in the state of the system are sufficient to give it a different dynamical path that can lead to much larger differences. For example, Stevens (1996) and Stevens et al. (1998) performed a number of experiments in which they varied only the random seed for the temperature perturbation that was used to initiate the model. Even this seemingly minor change resulted in differences in LWP as high as 20%. Viewed in this light, the differences in the LWP field between bin and parameterized microphysics runs for the higher drizzle case (Fig. 4) are quite reasonable; at 300 min simulation time the difference is only 4.5% and at 360 min, 20%. Over the course of the 6-h run, the difference is 4%. For the weaker drizzle case, agreement is excellent. For this reason comparison in a time-by-time, or point-by-point sense provides little insight and results have been presented in the form of (a) time series of domain (or cloud) averaged quantities, and (b) profiles of layer- and time-averaged profiles superimposed with 1-h averages to indicate variability. When viewed in this way, the results give us a better sense of the similarities and differences.

5.1. Sensitivity to breadth parameters

A number of experiments were performed in which the value of the breadth parameters (σ_g, the geometric standard deviation) of the lognormal distributions for the cloud and drizzle spectra were varied over a range of values ($1.15 < \sigma_g < 1.4$). Model runs were not very sensitive to σ_g, and did not change the essence of the results presented in Section 4. For given combinations of σ_g it is possible to modify drizzle production although this was found to be somewhat unpredictable owing to the dynamic nature of the system, as described above. An additional two predictive equations for an additional moment in each of the cloud and drizzle spectra might improve model performance, and this option is being explored. The possible improvement in results from such a model would have to be weighed against the additional computational expense.

5.2. Sensitivity to the representation of sedimentation

A sensitivity run was performed that was identical to the higher drizzle, P75 run with the exception of a simplified sedimentation scheme in which each of the cloud and drizzle modes was allowed to fall at the terminal velocity associated with the mass-mean of the spectrum. The time series from this run are shown in Fig. 7 and again compared

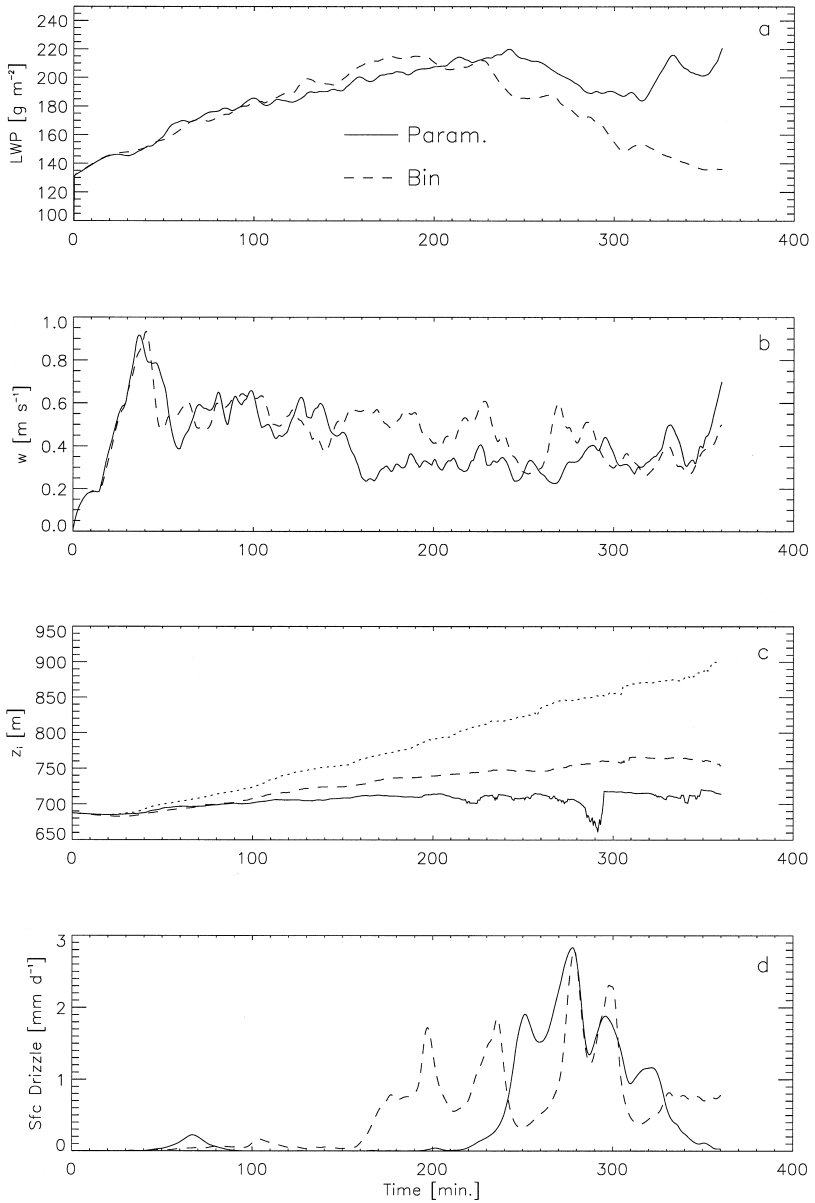

Fig. 7. As in Fig. 4, but for parameterized microphysics that uses the simplified sedimentation scheme described in the text.

with the bin model results. A degradation in results is immediately apparent: although LWPs track well for the first 220 min, they begin to diverge soon after, and by 360 min, they differ substantially. Between 150 min and 290 min, the turbulence levels in the

parameterized model are suppressed. The BL top exhibits markedly different behavior from that in the bin microphysical run. Surface drizzle values are the correct order of magnitude but the onset of drizzle is substantially delayed. Select profiles (Fig. 8) indicate significant differences between bin and parameterized microphysics both quantitatively and qualitatively. Drop-number concentrations are too low in-cloud and elevated below cloud, resulting in effective radii that are far too low below cloud. The drizzle flux profiles indicate in-cloud fluxes that are much too high. In Fig. 9, the profile of $w'w'$ also differs substantially from that of B75. The profile is rather flat and surface drizzle has, on the average, not reduced $w'w'$ and created the in-cloud peak characteristic of the B75 and P75 profiles.

This experiment builds on the results of Feingold et al. (1996a) where it was shown that even neglect of sedimentation of cloud droplets can affect precipitation formation. It provides further evidence that sedimentation is an important process in stratocumulus

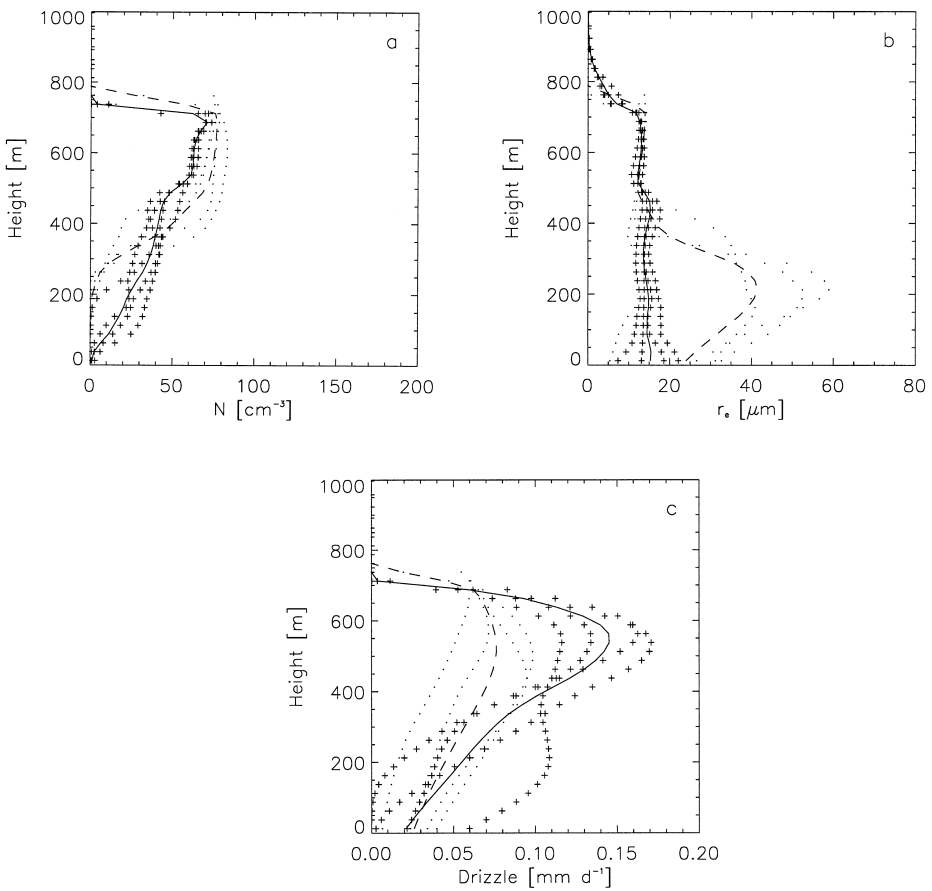

Fig. 8. Temporally and spatially averaged profiles of (a) N, (b) r_e, and (c) drizzle rate for the stronger drizzle case. The parameterization uses a simple sedimentation scheme.

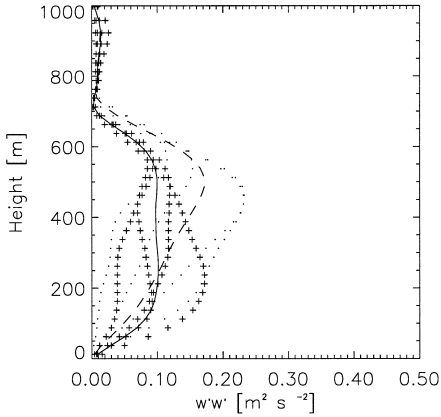

Fig. 9. Temporally and spatially averaged profiles of $w'w'$ where the parameterization uses a simple sedimentation scheme.

that requires more accurate treatment than a simple sedimentation of all drops at the mass-mean velocity.

6. Summary and conclusions

The development of a new microphysical parameterization scheme designed to capture the essence of a bin microphysical scheme but with significantly lower computational expense has been presented. The scheme uses a double basis function (lognormal) representation of the drop spectra and carries a total of four prognostic variables (mass and number of drops for each of the cloud and drizzle/rain spectra). A constant breadth is assumed for each of the spectra. The new approach differs from other parameterizations that use basis functions in that it accounts for the detailed bin interactions for collection and also allows for a differential (size-dependent) sedimentation. Efficiency is enhanced through the use of look-up tables that are prepared once, at the beginning of a simulation.

Results of microphysical fields as well as BL response to drizzle compare well with those of a detailed bin-microphysical scheme coupled with the same model. A sensitivity test using the proposed scheme but with a simplified sedimentation scheme showed significant degradation in results, illustrating the importance of this process in stratocumulus clouds.

Although the scheme has been applied here to a 2-D simulation of a stratocumulus cloud, it is suitable for multidimensional simulation of any warm convective cloud. It is also currently being extended to include treatment of the ice phase. The scheme has been developed with the recognition that although bin microphysical schemes represent the best means of representing cloud microphysics, the enormous computational expense of carrying the additional scalars (on the order of 50) renders large scale simulations at high resolution impossible on current machines. This problem is perhaps manageable for

the warm phase (e.g., Stevens, 1996) but quickly becomes unmanageable when simulations are extended to the ice phase. There the different ice species (pristine ice, graupel, snow, etc.) each require bin representation, and the number of required scalars extends to a few hundred. Because of the importance of maintaining an adequate representation of the model dynamics simultaneous with good microphysical treatment, reducing the model to 1-D is not a viable approach. Thus, the need for an efficient, accurate microphysical parameterization is great.

The work presented here exhibits good agreement between parameterized and bin microphysics; nevertheless, there is room for improvement. Current work is aimed at refinement of the scheme and application to other cloud types.

Acknowledgements

Support for this work came from NSF grant #ATM-9529321 entitled 'Simulations of cloud/radiative responses to variations in cloud condensation nuclei (CCN)'. Further support (GF) came from the Office of Naval Research #N00014-93-F0029 and the DOD/ISSO Lidar Wind Program. We thank Dr. Peter Duynkerke (Netherlands) for setting up the initial conditions used for the GCSS model intercomparison (1996) and steering the GCSS Stratocumulus Working Group.

Appendix A. Collection tables

The lookup table proves to be most compact if generated in three separate parts representing cloud–cloud, cloud–rain, and rain–rain collections individually. This is done by filling the full spectrum of bins from the sum of the cloud and rain distribution functions, defining a cutoff size at approximately 25 μm (radius) to distinguish droplet size bins that are considered cloud from those considered rain, and selectively zeroing portions of the collection kernel so that only an individual interaction type remains. The stochastic collection bin equation is solved with the partial kernel for each interaction for a unit period of time (1 s), and the resultant changes in mass and number of the cloud and rain bins are evaluated and entered into the table. This process is repeated for many values of the two independent parameters (number and mean mass) of the original cloud and rain distribution functions to produce table values for any situation encountered in a numerical simulation.

Cloud–cloud collections cause a transfer of mass from cloud to rain, a loss of cloud number, and a gain of rain number. The rates at which these occur are all proportional to the square of cloud number, a simple analytic relation which precludes the need for precomputation and table lookup. However, the rates are all complicated functions of cloud droplet mean mass. Thus, a one-dimensional table is constructed for each rate for a range of cloud droplet mean masses. The rates in the tables are normalized to unit cloud number concentration. During a model simulation, a table entry is accessed for the mean droplet mass in a given grid cell at a given timestep, and this entry is multiplied by cloud number squared to get the actual rate of number or mixing ratio gain or loss.

Accuracy in accessing table values may be increased by storing the log of the rates in the table and by linear interpolation from the table. However, given that the table is one-dimensional, there is negligible computational memory cost of storing 500 values in the table, and access of such closely spaced values without interpolation or taking the antilog is both very efficient and sufficiently accurate.

Cloud–rain interactions cause a transfer of mass from cloud to rain and a loss of cloud number but no change in rain number. The rates are proportional to cloud number but are complicated functions of cloud mass and rain number and mass. Thus, two tables are generated as a function of three variables. To maximize accuracy without requiring unduly large tables, table entries are the logarithm of the mass and number changes. Entries are linearly interpolated from the mass rate table over cloud droplet mass and rain number and from the cloud number rate table in rain number. Direct access of the nearest mass table value in rain mass and of the nearest number table value in cloud mass and rain mass is sufficiently accurate.

Rain–rain interactions cause a change only in rain number at a rate that depends on both rain mass and number. Thus, a single 2-dimensional table is constructed and interpolation from the table is in both directions. Once again, table entries are logarithms of the actual rate to improve linear interpolation accuracy.

Appendix B. Sedimentation tables (semi-Lagrangian)

The lookup tables, one for mass and one for number, are functions of three variables: source level (i.e., the vertical grid cell index where the condensate falls from on the current timestep), displacement number (the number of levels that condensate might fall in the current timestep), and a generalized distance that a hydrometeor of mean mass falls in one timestep. In general, some of the condensate (the smallest) will remain in the source grid cell, and some will fall one, two, or more grid cells in the current timestep. The table entries are the fraction of condensate mass or number from the source grid cell that falls into each grid cell beneath it.

The model can use terrain-following coordinates (although simulations here are over the ocean) that remain constant over all columns, both the number of model levels and the relative spacing between levels, but reduce the thickness of all levels in a column by a factor $C < 1$ over higher terrain. The generalized sedimentation fall distance is an actual fall distance divided by C. In other words, reduction of model level thickness over high topography is equivalent to increased fall velocity (of larger mean hydrometeor mass or due to lower air density) in determining how the mass and number of hydrometeors are distributed into model levels below the level from which they fall, and all effects can be combined into one table variable. The fall velocity of all other sizes of hydrometeors relative to that of the mean mass is fixed in time because the distribution function, spectral width, and terminal velocity function of mass are all fixed.

During model runtime for each grid cell, the generalized sedimentation fall distance is evaluated from the mean hydrometeor mass, the air density, and the factor C, and the mass and number from that cell are divided according to the fractional amounts indicated in the tables among the destination grid cells below. An additional table

indicating the lowest destination cell is also used for efficiency to prevent looping over unnecessary destination cells.

References

Albrecht, B.A., Bretherton, C.S., Johnson, D., Schubert, W.H., Frisch, A.S., 1995. The atlantic stratocumulus transition experiment—ASTEX. Bull. Am. Meteor. Soc. 76, 889–904.

Bechtold, P., Krueger, S.K., Lewellen, W.S., van Meijgaard, E., Moeng, C.-H., Randall, D.A., van Ulden, A., Wang, S., 1996. Modeling a stratocumulus topped PBL. Intercomparison among different one-dimensional codes and with LES. Bull. Am. Meteor. Soc. 77, 2033–2042.

Berry, E.X., 1967. Cloud droplet growth by coalescence. J. Atmos. Sci. 24, 688–701.

Berry, E.X., Reinhardt, R.L., 1974. An analysis of cloud droplet growth by coalescence. J. Atmos. Sci. 31, 1814.

Beheng, K., 1994. A parameterization of warm cloud microphysical conversion processes. Atmos. Res. 33, 193–206.

Boers, B., Jensen, J.B., Krummel, P.B., Gerber, H., 1996. Microphysical and short-wave radiative structure of wintertime stratocumulus clouds over the Southern Ocean. Q. J. Roy. Meteor. Soc., In press.

Bretherton, C.S., Pincus, R., 1995a. Cloudiness and marine boundary layer dynamics in the ASTEX Lagrangian experiment: I. synoptic setting and vertical structure. J. Atmos. Sci. 52, 2707–2723.

Bretherton, C.S., Austin, P., Siems, S.T., 1995b. Cloudiness and Marine boundary layer dynamics in the ASTEX Lagrangian experiment: II. Drizzle, surface fluxes and entrainment. J. Atmos. Sci. 52, 2724–2735.

Clark, T.L., 1973. Numerical modeling of the dynamics and microphysics of warm cumulus convection. J. Atmos. Sci. 30, 857–878.

Clark, T.L., 1976. Use of log-normal distributions for numerical calculation of condensation and collection. J. Atmos. Sci. 33, 810–821.

Cotton, W.R., Anthes, R.A., 1989. Storm and Cloud Dynamics. Academic Press, San Diego, 883 pp.

Cotton, W.R., Stevens, B., Nebuda, S., 1995. A question of balance-simulating microphysics and dynamics. Proc. Conf. Cloud Physics, January 15–20, Dallas, TX, Am. Meteor. Soc.

Duynkerke, P.G., Zhang, H., Jonker, P.J., 1995. Microphysical and turbulent structure of nocturnal stratocumulus as observed during ASTEX. J. Atmos. Sci. 52, 2763–2777.

Feingold, G., Stevens, B., Cotton, W.R., Walko, R.L., 1994. An explicit cloud microphysical/LES model designed to simulate the Twomey effect. Atmos. Res. 33, 207–233.

Feingold, G., Stevens, B., Cotton, W.R., Frisch, A.S., 1996a. On the relationship between drop in-cloud residence time and drizzle production in numerically simulated stratocumulus clouds. J. Atmos. Sci. 53, 1108–1122.

Feingold, G., Kreidenweis, S.M., Stevens, B., Cotton, W.R., 1996b. Numerical simulation of stratocumulus processing of cloud condensation nuclei through collision-coalescence. J. Geophys. Res. 101, 21391–21402.

Hall, W.D., 1980. A detailed microphysical model within a two-×dimensional dynamical framework: model description and preliminary results. J. Atmos. Sci. 37, 2486–2507.

Kessler, E., 1969. On the distribution and continuity of water substance in atmospheric circulation. Meteorological Monographs, 10: Am. Meteor. Soc., Boston, MA, 84 pp.

Kogan, Y.L., Lilly, D.K., Kogan, Z.N., Filyushkin, V.V., 1994. The effect of CCN regeneration on the evolution of stratocumulus layers. Atmos. Res. 33, 137–150.

Kogan, Y.L., Khairoutdinov, M.P., Lilly, D.K., Kogan, Z.N., Liu, Q., 1995. Modelling of stratocumulus cloud layers in a large eddy simulation model with explicit microphysics. J. Atmos. Sci. 52, 2923–2940.

Long, A.B., 1974. Solutions to the droplet collection equation for polynomial kernels. J. Atmos. Sci. 31, 1040–1052.

Louis, J.F., 1979. A parametric model of vertical eddy fluxes in the atmosphere. Boundary-Layer Meteor. 17, 187–202.

Moeng, C.-H., 1986. Large-eddy simulation of a stratus-topped boundary layer: I. Structure and budget. J. Atmos. Sci. 43, 2886–2900.

Moeng, C.-H., Cotton, W.R., Bretherton, C.S., Chlond, A., Khairoutdinov, M., Krueger, S., Lewellen, W., Mac Vean, M.K., Pasquier, J., Rand, H.A., Siebesma, A.P., Stevens, B., Sykes, R.I., 1996. Simulation of a stratocumulus-topped PBL: intercomparison among different numerical codes. Bull. Am. Meteor. Soc. 77, 261–278.

Olsson, P.Q., Feingold, G., Harrington, J., Cotton, W.R., Kreidenweis, S.M., 1996. Cloud resolving simulations of warm-season arctic stratus clouds. 12th Intnl. Conf. Clouds and Precip., Zurich, Switzerland, 19–23 Aug., pp. 752–755.

Pielke, R.A., Cotton, W.R., Walko, R.L., Tremback, C.J., Lyons, W.A., Grasso, L.D., Nicholls, M.E., Moran, M.D., Wesley, D.A., Lee, T.J., Copeland, J.H., 1992. A comprehensive meteorological modeling system—RAMS. Meteor. Atmos. Phys. 49, 69–91.

Stevens, B., 1996. On the dynamics of precipitating stratocumulus. PhD Thesis, Colorado State University, Fort Collins, CO 80523, USA, 140 pp.

Stevens, B., Feingold, G., Cotton, W.R., Walko, R.L., 1996a. On elements of the microphysical structure of numerically simulated stratocumulus. J. Atmos. Sci. 53, 980–1006.

Stevens, B., Walko, R.L., Cotton, W.R., Feingold, G., 1996b. A note on the spurious production of cloud edge supersaturations by Eulerian models. Mon. Wea. Rev. 124, 1034–1041.

Stevens, B., Cotton, W.R., Feingold, G., 1998. A critique of one- and two-dimensional models of boundary layer clouds with a binned representations of drop microphysics. Atmos. Res. 47–48, 529–553.

Twomey, S., 1959. The nuclei of natural cloud formation: II. The supersaturation in natural clouds and the variation of cloud droplet concentration. Geofis. Pura Appl. 43, 243–249.

Tzivion, S., Feingold, G., Levin, Z., 1987. An efficient numerical solution to the stochastic collection equation. J. Atmos. Sci. 44, 3139–3149.

Wyant, M.C., Bretherton, C.S., Rand, H., Stevens, D., 1997. Numerical simulations and conceptual model of the stratocumulus to trade cumulus transition. J. Atmos. Sci., in press.

Yair, Y., Levin, Z., Tzivion, S., 1994. Microphysical processes and dynamics of a Jovian thundercloud. Icarus 114, 278–299.